

Two Strategies on Border Labeling applied to the Estimation of Ejection Fraction

Oscar G. Panyella¹, Antonio Susin²

¹Departament de Tecnologies Audiovisuals, Enginyeria La Salle (URL), Barcelona, Spain, e-mail: oscarg@salleurl.edu

²Departament Matemàtica Aplicada I, Universitat Politècnica de Catalunya, Barcelona, Spain, e-mail: toni.susin@upc.es

Abstract—As we have already presented in previous conferences, our algorithm uses SPECT data to automatically recover the three-dimensional shape of the human's left ventricle. The reconstruction of both the internal (endocardium) and external (epicardium) surfaces, allows us to present a synthetic cardiac cycle for an actual patient and derive its associated ejection fraction estimation. In this paper, we complement our MLC filter methodology with another paradigm, the Discreet Contour Deformation Model. A comparison between ejection fraction values is presented, regarding both methods.

Index Terms— Tele-medicine, deformable models, virtual reality, image filters, 3D surface.

I. INTRODUCTION

This contribution is embedded inside a global project where a computerized system is intended to improve the analysis of the cardiac data defined by specialists.

When detecting a cardiac abnormality, there is different information to take into consideration: morphology, functionality and muscle irrigation plus vascular structure. In order to determine the pathologies, it is compulsory to perform quantitative and qualitative analysis for each of that information. A better diagnosis can be given to the patient if the related data are presented in an effective, accurate and understanding manner for the physician. Once the diagnosis has been determined, specialists define the patterns regarding the treatment of the patient. Then it comes clear that a simulation-oriented tool can be quite useful in order to practice quirurgical operations and predict their consequences. The virtual environment must be close to reality in the sense that it should give real sensations to the physicians, when manipulating a reconstructed heart.

II. MLC FILTER AND 3D DEFORMATION

We need to classify the pixels in our initial slice dataset (SPECT) according to some probability. This probability states if a pixel corresponds to the muscular tissue of the left ventricle.

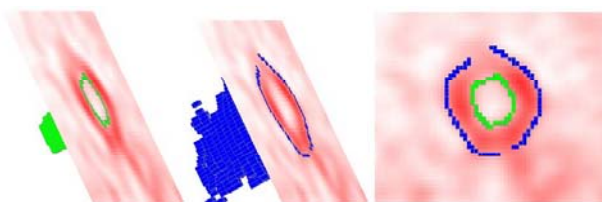


Fig. 1 The segmented left ventricle. From left to right: internal (3D), external (3D) and both borders (2D).

Given a data slice, there are several generic segmentation methods [1,5], that detect gradient changes, that can be used as the first sight to the edges that we are looking for.

Nevertheless we need some decision rules in order to classify them as belonging to one of the possible classes: external border, internal border or none (see fig. 1).

Our MLC approach [2] serves as a reliable classification tool. Our implementation finds automatically:

- The smallest circle that can be used as a noise removal tool for all the slices. This circle should be more accurate than the manual one defined by physicians.
- The division slice that identifies the beginning of the left ventricle's apex. This slice is first calculated and refined later using vertical coherence.

The algorithm ensures robustness because it performs all the calculations automatically, with no need of symmetry assumptions that might not be achievable due to the input dataset.

Fig. 2 presents some results obtained with the MLC filtering algorithm. As it shows, the borders have been correctly detected and labeled.

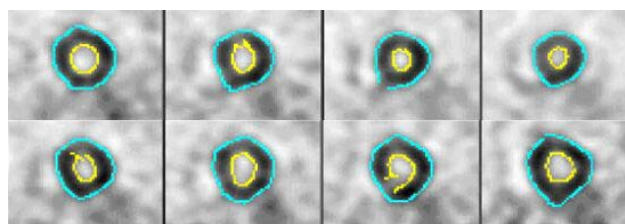


Fig. 2 Slice 15 of the same patient during a complete cardiac cycle data set.

The acquisition shown in fig. 2 consists on eight captures ranging from systole to diastole. Typical durations for the MLC filtering process are between one and two seconds long (1.48 seconds for every static instant of fig. 2, 23.74 seconds in total for all the slices). Each static dataset consists on 94208 voxels (64 x 64 pixels for 23 slices).

After the 2D labeling of the borders, we use particle systems in a Newtonian evolution scheme as a 3D segmentation tool. In that context, we have experimented with several methodologies available in terms of internal forces designed for 2D contours and 3D surfaces. We have successfully implemented *stretching* (controls the magnitudes associated to the sides of a given triangle), *shear* (acts on the inner triangle's angle), *bending* (defined between pairs of adjacent triangles) and *local curvature control* (minimization of the local curvature).

The internal forces might be used or not, depending on the deformation scheme applied: *plain deformation model*, a complex scheme where each of the triangles in the mesh has its own three elasticity forces; *spring-mass deformation model*, a well-known one where the only internal force is stretch, defined between pairs of particles; *restricted spring-mass deformation model*, which can be considered also as a contribution, where spring-forces are only allowed in the normal direction of the derived vector field and finally, *free deformation model*, where the only existing force is the external one, derived from the dataset. In that case, there is no connectivity between particles and topology must be maintained using a smoothing algorithm that has been developed entirely [3].

For the damping factors necessary in a simulation framework, we have also introduced the concept of damping maps that link a damping value with a voxel attending to its quality of data border.

Regarding the external force that attracts the surfaces to the data of interest, we use the *Gradient Vector Flow* [6] which is a vector field where the external force consists on the minimization of a functional that mixes the information derived from the image-intensities gradient with a diffusion term that allows the field to be spread out. This vector field solves two key difficulties: it avoids the need for the initial model to be close to the data to recover and it performs effectively within boundary concavities.

III. AUTOMATIC CONTOURING AND TESSELLATION OF THE 3D SHAPE WITH THE DISCREET CONTOUR DEFORMATION MODEL

The *Discreet Contour Deformation Model* is related to the minimization of the local curvature in order to balance the action of the external forces that model the

contour to follow all the variations that the energy related to the image demands [4]. It is important to note that in this case we are dealing with curves while in the previous methodology; we were defining forces related to triangulated surfaces.

When working with local curvature internal forces a suitable external force can be derived from a distribution of an external potential energy. This distribution can be associated to several characteristics of the image. One of the characteristics that best fits a good behavior, is the gray level and the gradient magnitude at every pixel (or voxel if working in a 3D framework).

If we need the model to follow the maximal gradient path through the image, we can use its magnitude and define an energy distribution proportional to its value. The implementation of the deformation process will try to drive all the vertices through the minimal energy areas. Moreover, the path for the contour is described by minimal energies (valleys) then we must invert the potential energy distribution.

This deformation model can be extended to a 3D framework and we can use this method to derive 3D surfaces of the left ventricle walls. In fact, it can be used as a new tessellation method.

The process consists on finding a first contour by the usual method. This contour will be used as an initial template for the rest of the slices. The process is described below:

- Begin by finding the 2D contour for the best slice (in terms of property intensity).
- Use this contour as a template for the neighbor slices (top and bottom).
- Repeat the process for all the slices in increasing and decreasing order, using the immediate contour as the initial template for the present contouring.
- Once the system has found all the contours, tessellate a 3D mesh along them.
- Close the boundaries of the mesh in the top and bottom contours. This will ensure that volume evaluations are correct.
- Smooth the mesh if needed.

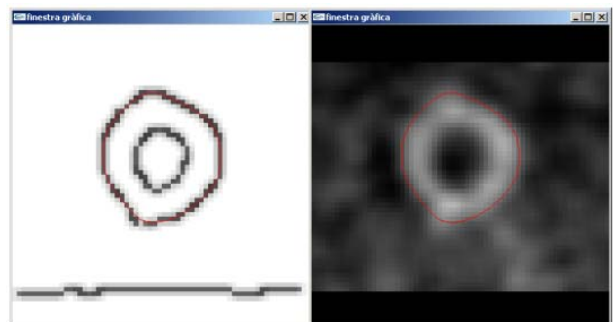


Fig. 3 Template contour for the discreet contour deformation model.

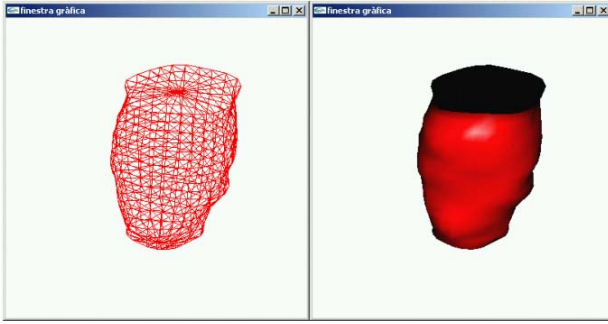


Fig. 4 3D recreation of the external surface by the discrete contour tessellation method.

Fig. 3 presents the template contour for a test using actual patient's data (external surface tessellation). The initial contour was found in the slice 16 of the dataset (out of 23), considered to be representative enough in terms of quality and intensity.

From that initial contour, the whole dataset can be segmented by applying the previously described algorithm, while maintaining vertical coherence.

Once the whole dataset has been segmented in 2D, we apply our tessellation strategy in order to build the 3D surface that we are looking for, as stated in fig. 4.

IV. COMPARATIVE ON EJECTION FRACTION ESTIMATIONS

Table 1 and fig. 5 present a complete cardiac cycle reconstruction, recovered from actual patient's data by using border labeling with the MLC filter plus Newtonian evolution. The cycle is formed by eight temporal acquisitions. Each data set consists on $64 \times 64 \times 24$ voxels, with spatial resolutions of 2,87 mm (X), 2,87 mm (Y) and 5,74 mm (Z).

Table 1 Volumes for the eight temporal instances for the MLC filter labeling plus the Newtonian evolution scheme.

| | 1 | 2 | 3 | 4 |
|-------------|--------|--------|--------|--------|
| Int. | 74741 | 45677 | 36523 | 32956 |
| Ext. | 443762 | 316804 | 254112 | 250131 |
| Wall | 369021 | 271127 | 217589 | 217175 |
| | 5 | 6 | 7 | 8 |
| Int. | 47237 | 55825 | 63133 | 79581 |
| Ext. | 299779 | 345830 | 451525 | 473608 |
| Wall | 252542 | 290005 | 388392 | 394027 |

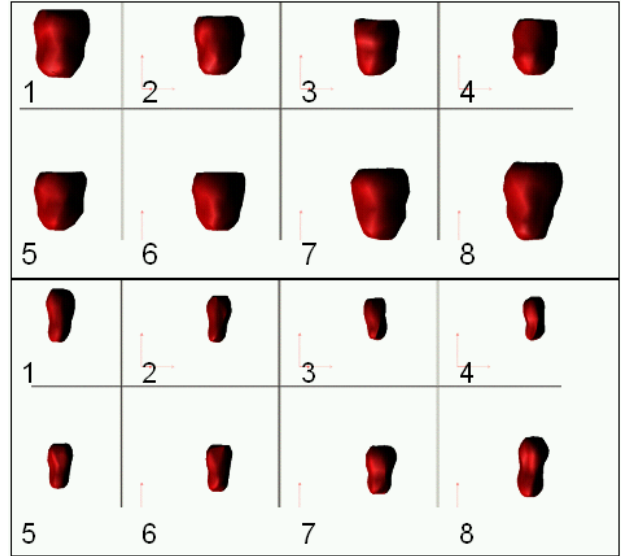


Fig. 5 The cardiac cycle retrieved by the MLC filter labeling plus the Newtonian evolution scheme.

The meshes were generated using the free deformation model with a Runge Kutta 4 explicit numerical method, using a stepsize of 0,1 seconds.

One can notice the changes in volume (mm^3) as the organ beats (from systole to diastole), here noticeable as the sequence defines a complete cardiac cycle.

The ejection fraction (EF) can be calculated for this ventricle as equation 1 shows. In there all the volumes are internal. As it is showed, its value is inside the interval 50% - 70% which states for a non-pathological situation. Moreover, physician's 2D software gave an ejection fraction value of 53% for this case which is really close to our computation with this method.

$$\begin{aligned}
 EF &= \frac{\text{DiastoleEndVolume} - \text{SystoleEndVolume}}{\text{DiastoleEndVolume}} \\
 &= \frac{79581 - 32956}{79581} = 0.586 \Rightarrow 58.6\%
 \end{aligned} \tag{1}$$

We can also apply the discrete contour methodology to the reconstruction of the cardiac cycle. Fig. 6 shows the external and internal meshes retrieved for the same dataset but when using this different approach. Rows one and two correspond to the external surfaces and rows three and four to the internal ones. We can also evaluate the volumes and the ejection fraction. The results can be seen in table 2 and equation 2 respectively.

Compared to those in table 1, the volumes are inferior in absolute terms but the ejection fraction is practically equal. In that sense, we can state that this test retrieved lower volumes but as long as this fact is consistent in all the reconstructions, the ejection fraction, which is a relative parameter, can be considered as good as the previous one.

Table 2 Volumes for the eight temporal instances for the Discreet Contour Deformation Model.

| | 1 | 2 | 3 | 4 |
|-------------|--------|--------|--------|--------|
| Int. | 49973 | 29964 | 20849 | 18929 |
| Ext. | 349349 | 264170 | 215068 | 201387 |
| Wall | 299376 | 234206 | 194219 | 182458 |
| | 5 | 6 | 7 | 8 |
| Int. | 27440 | 40689 | 47080 | 49034 |
| Ext. | 247078 | 291363 | 322970 | 373602 |
| Wall | 219638 | 250674 | 275890 | 324568 |

For this concrete methodology, we find the volumes by calculating the area of each contour. We subtract the area of the first contour to these (*Green's theorem*) and we multiply the result by the thickness between slices. We add then all the partial volumes.

Then we have to evaluate the contributions of all the lateral triangles that link the different contours. The contribution for a triangle is calculated like the area that it projects multiplied by the slice thickness and divided by a factor of 2.

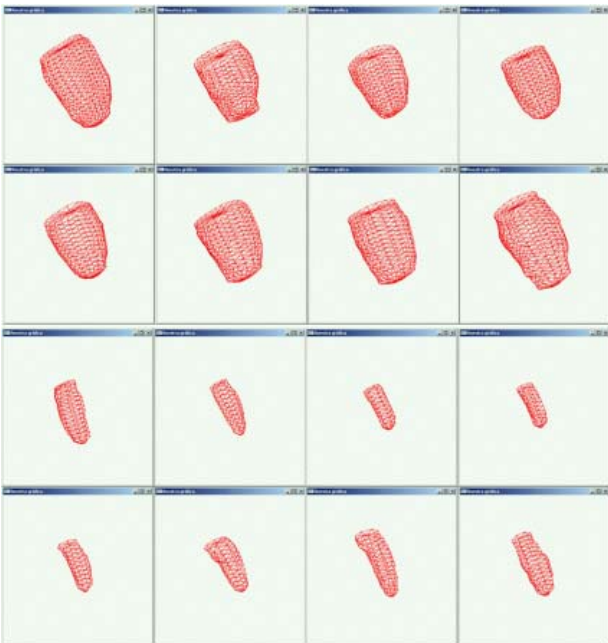


Fig. 6 The cardiac cycle retrieved by the Discreet Contour Deformation Model.

$$EF = \frac{DiastoleEndVolume - SystoleEndVolume}{DiastoleEndVolume} \quad (2)$$

$$= \frac{49973 - 18929}{49973} = 0.621 \Rightarrow 62.1\%$$

Depending on the sign of the normal vector, this contribution is added (positive normal) or subtracted (negative normal).

REFERENCES

This work has been partially financed by the TIC2000-1009 project. The first author is granted by an EPSON "Rosina Ribalta" prize.

The authors thank the medical applications research group at the IRI-UPC, the Nuclear Cardiology team at Vall d'Hebrón Hospitals and the people integrating the graphics & VR group at the Multimedia Section of La Salle School of Engineering.

- [1] J. Canny. "A Computational Approach to Edge Detection". *IEEE Transactions on Pattern Analysis and Machine Intelligence* 1986; 8(6):679-698.
- [2] O. García, A. Susin. "MLC filtering applied to the 3D reconstruction of the left ventricle". *CEIG 2003*, XIII Congreso Español de Informática Gráfica 2003;13:17-30.
- [3] O. García, *An Easy-to-code Smoothing Algorithm for 3D Reconstructed surfaces*, *Graphics Programming Methods*, Jeff Lander, Charles River Media (July 2003). ISBN: 1-58450-299-1. Pages 139 to 146.
- [4] S. Lobregt and M. A. Viergever, "A discrete dynamic contour model". *IEEE Trans. on Medical Imaging*, 14(1):12-24, March 1995.
- [5] M. Ruzon and C. Tomasi. "Color Edge Detection with the Compass Operator". *Proceedings of the IEEE Conference on Computer Vision and Pattern Recognition* 1999;2:160-166.
- [6] C. Xu and J.L. Prince, "Snakes, shapes, and gradient vector flow". *IEEE Transactions on Image Processing* 1998;7(3):359-369.